

Supplementary Information

Pressure and temperature sensing properties of $\text{Nd}^{3+}:\text{YTaO}_4$ luminescence

Pengyu Zhou,^{*a} Qingli Zhang,^b Xiuming Dou,^c Jian Wang,^c Baoquan Sun,^{*c} Yuhua Shen,^a Bao Liu^a
and Dandan Han^a

^a School of Science, Northeast Electric Power University, Jilin 132012, China.

^b Key Laboratory of Photonic Devices and Materials, Anhui Institute of Optics and Fine Mechanics, Chinese Academy of Sciences, Hefei 230031, China.

^c State Key Laboratory of Superlattices and Microstructures, Institute of Semiconductors, Chinese Academy of Sciences, Beijing 100083, China.

*Corresponding author: 20162715@neepu.edu.cn (Pengyu Zhou), bqsun@semi.ac.cn (Baoquan Sun).

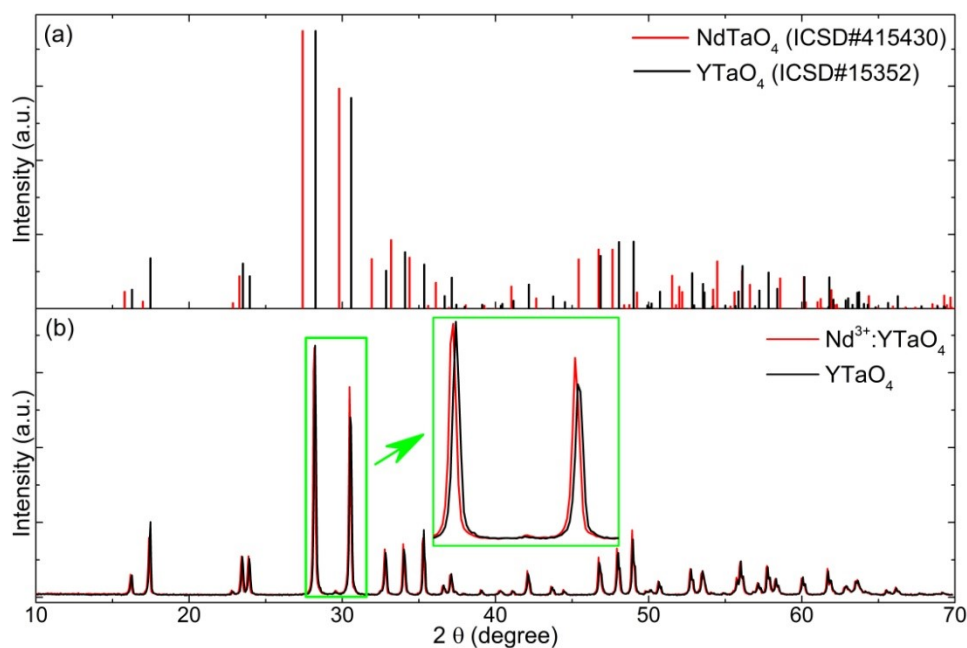


Fig. S1 (a) Comparison of the standard XRD patterns of M'-phase YTaO_4 and NdTaO_4 . (b) Comparison of the XRD patterns of the synthesized M'-phase YTaO_4 and $\text{Nd}^{3+}:\text{YTaO}_4$ samples. Inset is an enlarged view of the two highest diffraction peaks.

To better know the structural information of the samples, detailed comparisons among the XRD patterns of the synthesized samples and the corresponding standard XRD patterns were made, see Fig. S1. According to the research of Refs. 1 and 2, M'-phase NdTaO_4 and YTaO_4 both belong to the P2/a space group symmetry. The lattice parameters of M'-phase NdTaO_4 are¹: $a = 5.2437 \text{ \AA}$, $b = 5.5969 \text{ \AA}$, $c = 5.4275 \text{ \AA}$, $\alpha = \gamma = 90^\circ$, $\beta = 96.767^\circ$. The cell volume of M'-phase NdTaO_4 is 158.18 \AA^3 .¹ The lattice parameters of M'-phase YTaO_4 are²: $a = 5.2920 \text{ \AA}$, $b = 5.4510 \text{ \AA}$, $c = 5.1100 \text{ \AA}$, $\alpha = \gamma = 90^\circ$, $\beta = 96.440^\circ$. The cell volume of M'-phase YTaO_4 is 146.48 \AA^3 .² As Fig. S1(a) shows, XRD diffraction peaks of M'-phase NdTaO_4 and YTaO_4 are in one-to-one correspondence because of resemble structure. Moreover, all XRD diffraction peaks of M'-phase NdTaO_4 locate at lower degrees in comparison with those of M'-phase YTaO_4 , due to that the cell volume of M'-phase NdTaO_4 is larger than that of M'-phase YTaO_4 . As Fig. S1(b) shows, a similar relation can also be found between the XRD patterns of the synthesized M'-phase $\text{Nd}^{3+}:\text{YTaO}_4$ and YTaO_4 . Compared to YTaO_4 , all XRD diffraction peaks of $\text{Nd}^{3+}:\text{YTaO}_4$ shift a little to the lower degree side, reflecting an expansion of the host lattice induced by the Nd^{3+} doping vividly. This is a good evidence for Nd^{3+} ions entering into the host lattice.

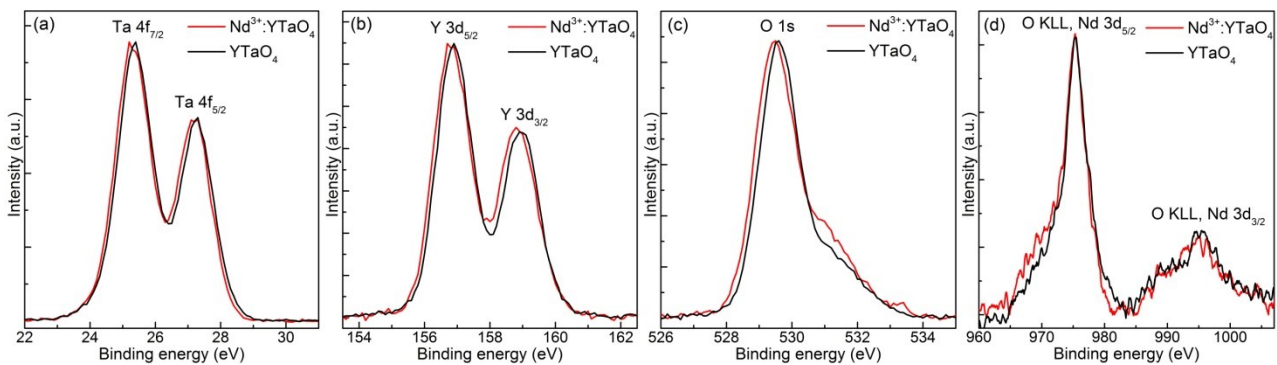


Fig. S2 Normalized Ta 4f (a), Y 3d (b), O 1s (c), O KLL and Nd 3d (d) XPS spectra for the M'-phase YTaO_4 and $\text{Nd}^{3+}:\text{YTaO}_4$ samples.

To further confirm that the Nd^{3+} ions were successfully doped into the host, a comparison of XPS spectra of the M'-phase $\text{Nd}^{3+}:\text{YTaO}_4$ and YTaO_4 samples was made. As Figs. S2(a) – (c) show, compared to the M'-phase YTaO_4 , Ta 4f, Y 3d and O 1s peaks of the M'-phase $\text{Nd}^{3+}:\text{YTaO}_4$ shift a little to the lower energy side, indicating the added Nd^{3+} ions indeed enter into the lattice of the host. It should be mentioned that, the Nd 3d peaks are the main evidence used for identifying the Nd^{3+} ions based on XPS³. Unfortunately, they highly overlap with the O KLL peaks³ (see Fig. S2(d)),

which brings huge difficulties for the analysis of the XPS spectra. Nevertheless, a little difference can also be found in the corresponding spectral comparison shown in Fig. S2(d).

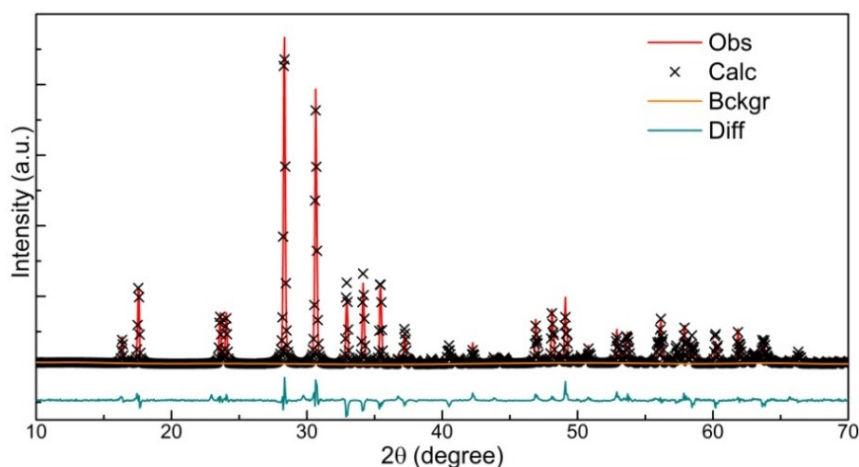


Fig. S3 Rietveld refinement results of the XRD data of the M'-phase Nd³⁺:YTaO₄ sample.

To know the detailed structure information of the M'-phase Nd³⁺:YTaO₄, the XRD data of M'-phase Nd³⁺:YTaO₄ was fitted using the Rietveld refinement method. The structure parameters of M'-phase YTaO₄ were taken as the initial values, the background function, lattice parameters, atomic coordinates, and isotropic temperature factors were refined with the software GSAS⁴. The corresponding refinement results are shown in Fig. S3 and Table S1.

Table S1 Structure parameters of the M'-phase Nd³⁺: YTaO₄ sample obtained using the Rietveld refinement method.

Atom	Site	<i>x</i>	<i>y</i>	<i>z</i>	<i>U</i> _{iso}
Nd	2e	0.25	0.8477	0.5	0.0081
Y	2e	0.25	0.7695	0.5	0.0444
Ta	2f	0.25	0.3049	0.0	0.0168
O1	4g	0.492	0.4355	0.2681	0.0633
O2	4g	0.081	0.069	0.2511	0.0581

Lattice parameters $a = 5.2996 \text{ \AA}$, $b = 5.4546 \text{ \AA}$, $c = 5.1132 \text{ \AA}$, $\alpha = \gamma = 90^\circ$, $\beta = 96.436^\circ$

space group: P2/a

R factors $R_p = 13.52\%$, $R_{wp} = 10.48\%$

The elemental analysis/chemical characterization performed by EDS confirms the presence of Nd, Y, Ta and O elements once again, see Fig. S4(a). A semi quantitative analysis of the elemental composition in atomic percent is also shown in the figure. To better investigate the distribution uniformity for each element, a area (see Fig. S4(b)), larger than that shown in Fig. 1(c), was randomly selected for EDS mapping characterization. As Figs. S4(c) – (f) show, Nd, Y, Ta and O atoms are evenly distributed throughout the sample.

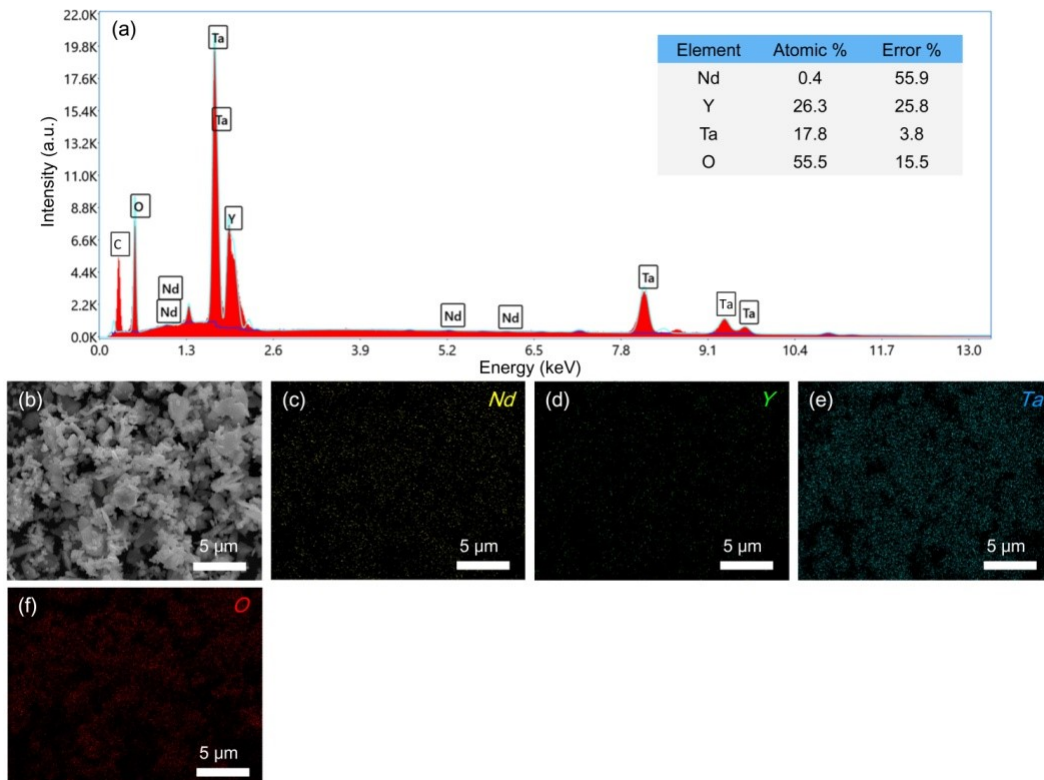


Fig. S4 EDS spectrum (a), SEM image (b) and element mapping (c) – (f) of the M'-phase $\text{Nd}^{3+}:\text{YTaO}_4$ sample.

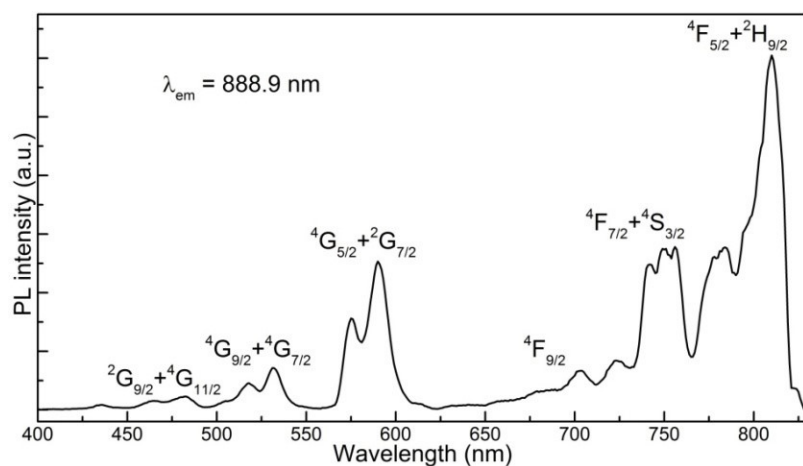


Fig. S5 Excitation spectrum of the M'-phase $\text{Nd}^{3+}:\text{YTaO}_4$ sample monitored at 888.9 nm.

For deeper investigation on a possible excitation process, PLE spectroscopy experiments were carried out on the M'-phase $\text{Nd}^{3+}:\text{YTaO}_4$ sample. Figure S5 shows the PLE spectrum of the M'-phase $\text{Nd}^{3+}:\text{YTaO}_4$ sample recorded by monitoring the highest emission line of ${}^4\text{F}_{3/2} \rightarrow {}^4\text{I}_{9/2}$ transition at 888.9 nm in the 400 – 830 nm range. The PLE spectrum exhibits Nd^{3+} excitation bands with centers at about 470, 530, 585, 700, 750 and 800 nm which correspond to the direct excitation of electrons from the ground state ${}^4\text{I}_{9/2}$ of Nd^{3+} to different excited states (see Figs. S5).

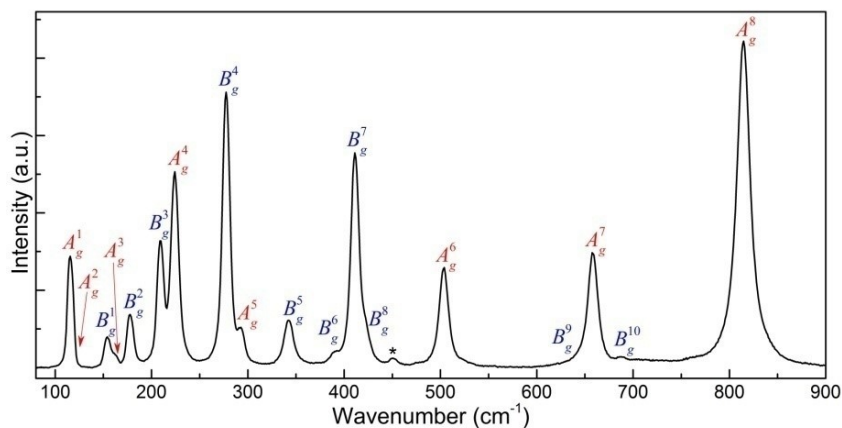


Fig. S6 Raman spectrum of the M'-phase YTaO_4 sample at ambient condition. Raman modes are labeled according to Ref. 5. The peak marked with asterisk may be an artifact due to electronic transition of Y^{3+} .

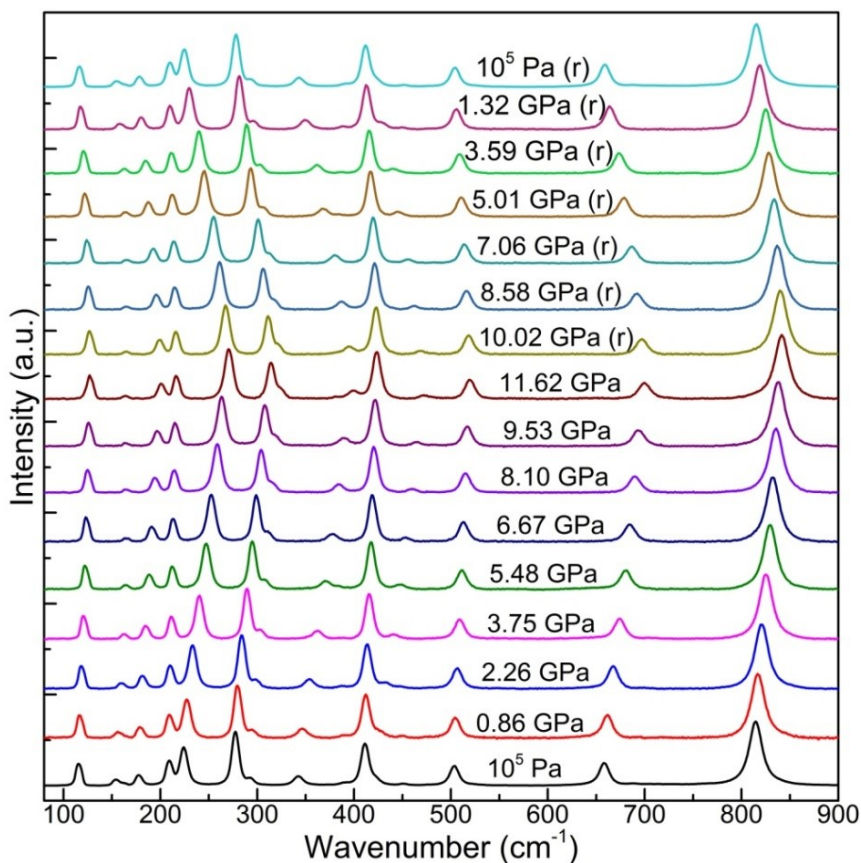


Fig. S7 Raman spectra of the M'-phase YTaO₄ sample at room temperature and various pressures. The spectra recorded in the process of releasing pressure are marked with (r).

The stability of the host material M'-phase YTaO₄ under high pressure was examined using Raman spectroscopy. Raman spectra of the M'-phase YTaO₄ at various pressures are shown in Figs. S6 and S7. According to the previous researches⁵, the M'-phase YTaO₄ should have 18 Raman-active modes (see Fig. S6) at the center of the Brillouin zone: $\Gamma = 8A_g + 10B_g$. The A_g and B_g modes represent parallel- and cross-polarized Raman scattering, respectively. As Fig. S7 shows, the Raman spectral evolution is continuous without any sign of phase transition, indicating the M'-phase structure of YTaO₄ is stable in the pressure range concerned in this research. Moreover, during the process of decompression down to ambient pressure, the Raman spectrum returns to the initial pattern, indicating the pressure-induced variation of the M'-phase structure of YTaO₄ is reversible.

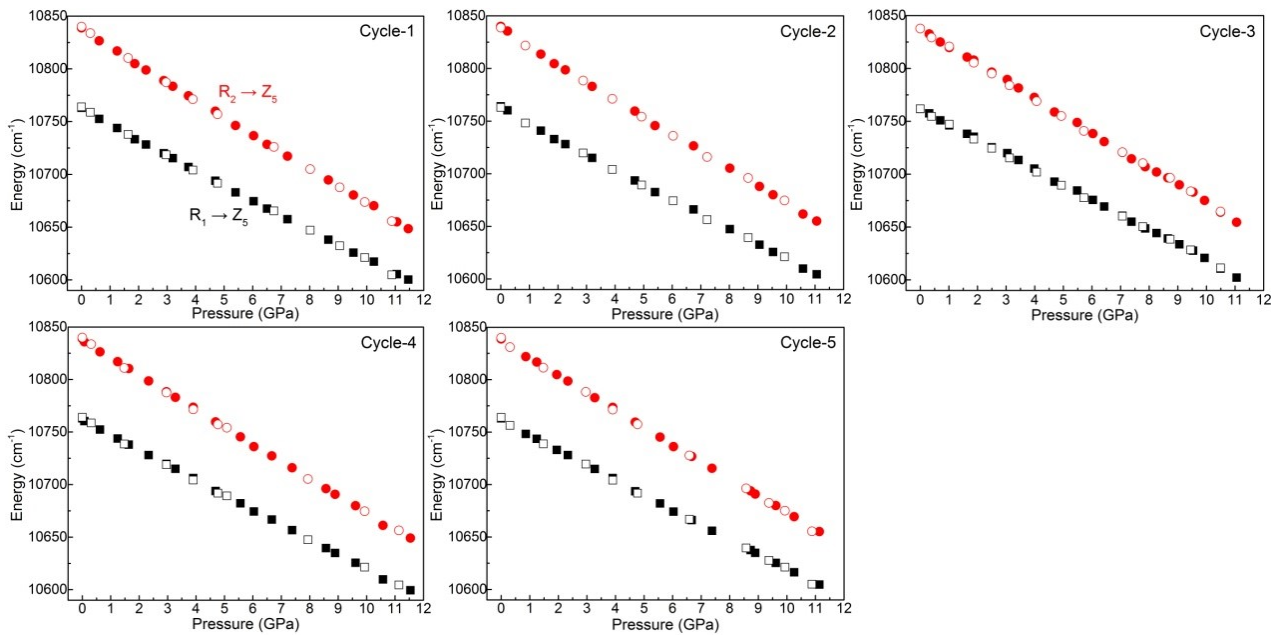


Fig. S8 Repeatability tests of spectral positions of R_{2,1} → Z₅ emission lines for the M'-phase Nd³⁺:YTaO₄ sample in a pressure range of 10⁵ Pa – 11.5 GPa and at room temperature. Solid dots represent data recorded in the pressure increasing process, open dots represent data recorded in the pressure releasing process.

To further discuss the feasibility of using M'-phase Nd³⁺:YTaO₄ for pressure sensing, pressure-recycle tests over five compression-decompression process were conducted on the present sample. As Fig. S8 shows, the two emission lines with the highest pressure sensitivities of M'-phase Nd³⁺:YTaO₄ exhibit excellent repeatability.

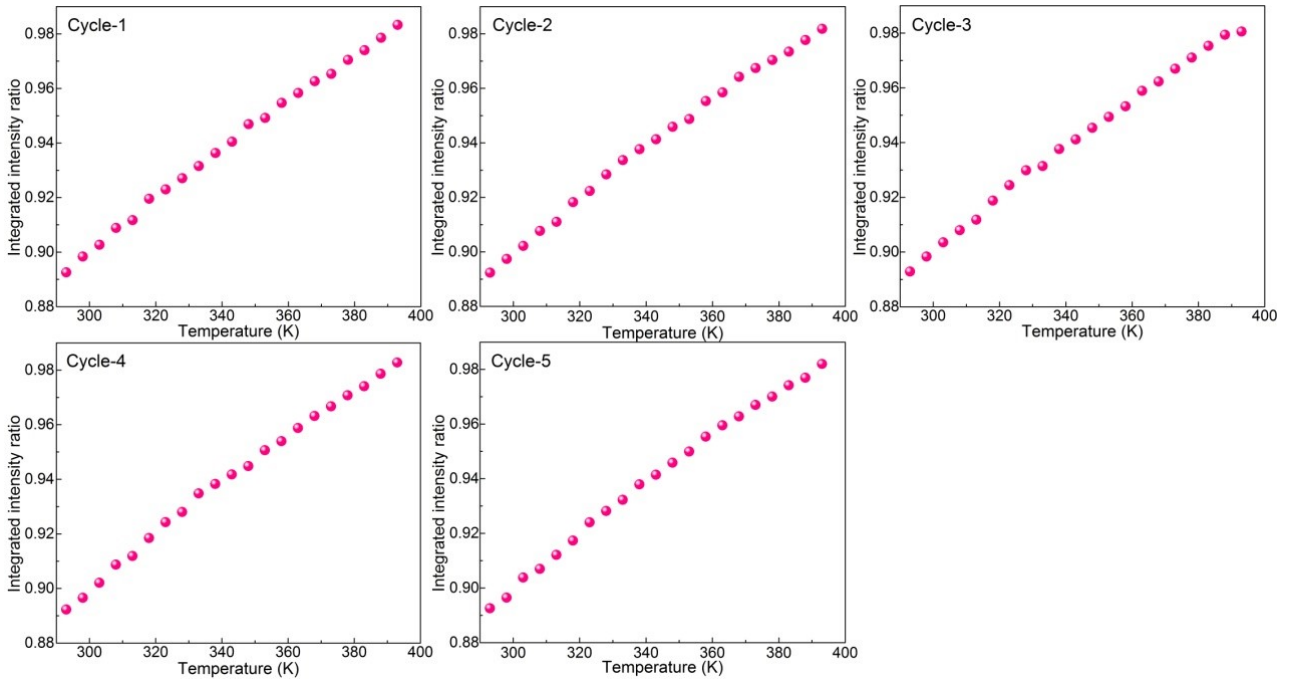


Fig. S9 Repeatability tests of the intensity ratio of $R_{2,1} \rightarrow Z_5$ emission lines for the M' -phase $\text{Nd}^{3+}:\text{YTaO}_4$ sample in a temperature range of 293 – 393 K and at ambient pressure.

To discuss the feasibility of using M' -phase $\text{Nd}^{3+}:\text{YTaO}_4$ for temperature sensing, temperature-recycle tests over five heating process were conducted on the present sample. As Fig. S9 shows, the intensity ratio I_2/I_1 of $R_{2,1} \rightarrow Z_5$ emission lines of the M' -phase $\text{Nd}^{3+}:\text{YTaO}_4$ exhibit excellent repeatability.

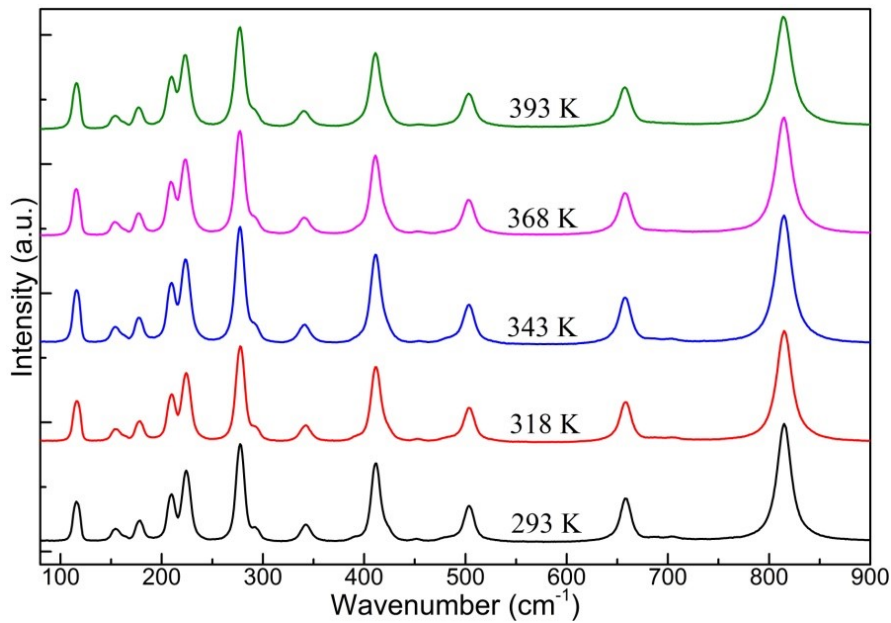


Fig. S10 Raman spectra of the M' -phase YTaO_4 sample at ambient pressure and various temperatures.

To further discuss the feasibility of the M'-phase Nd³⁺:YTaO₄ in application of temperature sensing, the thermal stability of the host material M'-phase YTaO₄ was examined using Raman spectroscopy. As Fig. S10 shows, all the Raman spectra recorded at the higher temperatures are highly consistent to that recorded at 293 K, indicating the M'-phase YTaO₄ is stable in the temperature range concerned in this research.

Reference

- 1 I. Hartenbach, F. Lissner, T. Nikelski, S. F. Meier, H. Mueller-Bunz and T. Schleid, *Z. Anorg. Allg. Chem.*, 2005, **631**, 2377 – 2382.
- 2 G. M. Wolten, *Acta Cryst.*, 1967, **23**, 939 – 944.
- 3 J. P. Baltrus and M. J. Keller, *Surf. Sci. Spectra*, 2019, **26**, 014001.
- 4 A. C. Larson and R. B. V. Dreele, *Los Alamos National Laboratory Report LAUR*, 2004, 86 – 748.
- 5 K. P. F. Siqueira, G. B. Carvalho and A. Dias, *Dalton Trans.*, 2011, **40**, 9454 – 9460.